IMMOBILIZED P-25 TiO_2/MONTMORILLONITE AND P-25 TiO_2/ORGANO-MONTMORILLONITE BILAYER SYSTEMS FOR THE SYNERGISTIC PHOTOCATALYTIC-ADSORPTION REMOVAL OF METHYLENE BLUE AND HUMIC ACID FROM AQUEOUS SOLUTIONS

NGOH YING SHIN

UNIVERSITI SAINS MALAYSIA

2015

IMMOBILIZED P-25 TiO_2/MONTMORILLONITE AND P-25 TiO_2/ORGANO-MONTMORILLONITE BILAYER SYSTEMS FOR THE SYNERGISTIC PHOTOCATALYTIC-ADSORPTION REMOVAL OF METHYLENE BLUE AND HUMIC ACID FROM AQUEOUS SOLUTIONS

by

NGOH YING SHIN

Thesis submitted in fulfilment of the requirements for the degree of Doctor of Philosophy

DECEMBER 2015

ACKNOWLEDGEMENT

Hereby, I would like to sincerely express my appreciation to those who have assisted me in one way or another for materializing this research and thesis.

First and foremost, I am deeply indebted to my research supervisor Professor Dr. Mohd. Asri Bin Mohd. Nawi for giving me the great opportunity to pursue postgraduate research under his supportive and inspiring mentorship. I am earnestly grateful to my supervisor whose selfless time, constructive guidance, invaluable advice and continuous encouragement in any situations have kept me going throughout my candidature.

I would also like to extend my utmost gratitude to Malaysia's Ministry of Higher Learning for providing me the MyPhD postgraduate scholarship under the MyBrain program. Much appreciation also goes to Universiti Sains Malaysia for funding the works in this research substantially through the USM Postgraduate Research Grant Scheme (PGRS: 1001/PKIMIA/844101). I am also thankful to the academic as well as supporting staff of USM's School of Chemical Sciences and Institute of Postgraduate Studies (IPS) for their professional services, technical supports and administrative assistances. My gratitude also goes out to all past and present colleagues within the research group for their friendships and co-operations.

Last but not least, I would like to convey my most heartfelt appreciation to my respected parents and sister for their unconditional love, unwavering support and tireless sacrifice in many ways throughout this journey. It has been an eye-opening and humbling learning experience and I am so thankful for all the help that I have received from individuals who have involved directly or indirectly in this research over the years.

TABLE OF CONTENTS

LIST OF TABLES

LIST OF FIGURES

LIST OF ABBREVIATIONS

AOPs	advanced oxidation processes
BET	Brunauer-Emmet-Teller
CB	conduction band
CEC	cation exchange capacity
COD	chemical oxygen demand
CPB	cetylpyridinium bromide
DOC	dissolved oxygen carbon
E_{bg}	Band gap energy
EDX	energy dispersion X-ray
ENR-50	epoxidized natural rubber of 50 % epoxidation
eV	electron volt
FE-SEM	field emission scanning electron microscope
FTIR-ATR	Fourier transform infrared - attenuated total reflectance
GC-MS	gas chromatography - mass spectrometry
GLA	glutaraldehyde
GPC	gel permeation chromatography
HA	humic acid
HDTMA-Br	hexadecyltrimethylammonium bromide
HPLC	high performance liquid chromatography
IEP	isoelectric point
IUPAC	International Union of Pure and Applied Chemistry
LC-MS	liquid chromatography - mass spectrometry
MB	methylene blue
MT	montmorillonite

MT-PVAB	montmorillonite-poly (vinyl) alcohol binder
MT-PVAB/GP	montmorillonite-poly (vinyl) alcohol binder immobilized on glass plate
O-MT	organo-montmorillonite
O-MT-PVAB/GP	organo-montmorillonite-poly (vinyl) alcohol binder immobilized on glass plate
O-MT-PVAB	organo-montmorillonite-poly (vinyl) alcohol binder
P-25 TiO_2	P-25 Degussa titanium (IV) oxide
PLS	photo-luminescence spectroscopy
PVA	poly (vinyl) alcohol
PVAB	poly (vinyl) alcohol binder
PVC	poly (vinyl) chloride
PZC	point of zero charge
TOC	total organic carbon
UV-vis DRS	ultraviolet-visible diffused reflectance spectroscopy
UV-vis	ultraviolet-visible
VB	valence band

SISTEM DWILAPISAN TERPEGUN P-25 TiO_2/MONTMORILONIT DAN P-25 TiO_2/ORGANO-MONTMORILONIT UNTUK PENYINGKIRAN SINERGISTIK FOTOPEMANGKINAN-PENJERAPAN METILENA BIRU DAN ASID HUMIK DARIPADA LARUTAN AKUEUS

ABSTRAK

Kajian ini memerihalkan pembangunan sistem dwilapisan terpegun P-25 TiO_2/montmorilonit dan P-25 TiO_2/organo-montmorilonit untuk penyingkiran sinergistik fotopemangkinan-penjerapan metilena biru (MB) dan asid humik (HA) daripada larutan akueus. Tahap awal pembangunan sistem dwilapisan terpegun tersebut melibatkan kajian terhadap sifat penjerapan bahan penjerap yang merupakan lapisan bawah sistem tersebut. Bahan penjerap terpegun montmorilonit (MT-PVAB/GP) disediakan untuk penjerapan MB manakala penjerap terpegun organo-montmorilonit (2.0-O-MT-PVAB/GP) direka untuk proses penjerapan HA. Pencirian MT-PVAB/GP dan 2.0-O-MT-PVAB/GP dilakukan dengan menggunakan mikroskop elektron imbasan pancaran medan (FE-SEM), sinar-X penyerakan tenaga (EDX), spektroskopi inframerah transformasi Fourier – pantulan keseluruhan dikecilkan (FTIR-ATR), proses penjerapan-penyaherapan N_2 dan pengukuran keupayaan zeta. Proses penjerapan MB dan HA dipengaruhi oleh muatan penjerap, pH larutan, kadar pengudaraan, kepekatan awal dan masa sentuhan. Data kinetik proses penjerapan MB dan HA didapati berpadanan dengan model pseudo-tertib-kedua dan kadar proses dikawal oleh pembauran intra-zarah. Proses penjerapan MB dan HA didapati mematuhi model Langmuir. Kapasiti penjerapan maksimum, q_m MT-PVAB/GP terhadap MB adalah sebanyak 111 mg g^{-1}. Nilai q_m untuk proses penjerapan HA pada UV_{254} dan $Colour_{436}$ adalah masing-masing 31.75 dan 29.59 mg

g^{-1}. Nilai parameter termodinamik menunjukkan proses penjerapan MB dan HA adalah lebih baik pada suhu tinggi, endoterma dan spontan. Bagi pemfabrikatan sistem dwilapisan terpegun, komposisi optimum lapisan bawah sama ada MT-PVAB/GP ataupun 2.0-O-MT-PVAB/GP dan lapisan atas P-25 TiO_2 masing-masing ditentukan melalui penyingkiran sinergistik MB dan HA secara fotopemangkinan-penjerapan. Pencirian sistem dwilapisan P-25 TiO_2/MT-PVAB/GP dan P-25 TiO_2/2.0-O-MT-PVAB/GP teroptimum dijalankan dengan menggunakan FE-SEM, EDX, spektroskopi kepantulan baur ultra lembayung-nampak (UV-vis DRS) dan spektroskopi fotopendarcahaya (PLS). Aktiviti fotopemangkinan-penjerapan sinergistik sistem dwilapisan terpegun adalah diterajui oleh kapasiti penjerapannya yang dipengaruhi oleh faktor pH larutan, kadar pengudaraan dan kepekatan awal larutan jerap; peningkatan kadar pemisahan pasangan elektron-lubang dan pengurangan jurang tenaga jalur berbanding dengan sistem satu lapisan P-25 TiO_2/GP. Keamatan sinaran UV juga mempengaruhi aktiviti fotopemangkinan sistem dwilapisan. Sistem dwilapisan P-25 TiO_2/MT-PVAB/GP menunjukkan kadar penyingkiran sinergistik fotopemangkinan-penjerapan MB adalah sebanyak 3.51 kali ganda lebih cepat berbanding P-25 TiO_2/GP. Lebih-lebih lagi, sistem dwilapisan P-25 TiO_2/MT-PVAB/GP sangat boleh diguna semula di mana secara purata, sistem ini dapat menyingkirkan 99.7 ± 0.14 % MB pada kadar 0.123 ± 0.006 min^{-1} sepanjang 10 kitaran ulang guna. Sistem dwilapisan P-25 TiO_2/2.0-O-MT-PVAB/GP pula mempamerkan peningkatan purata sebanyak 2.10 and 3.34 kali ganda dalam kadar penyingkiran sinergistik HA pada UV_{254} secara fotopemangkinan-penjerapan berbanding dengan P-25 TiO_2/MT-PVAB/GP dan P-25 TiO_2/GP. Sistem dwilapisan P-25 TiO_2/2.0-O-MT-PVAB/GP juga menunjukkan kebolehgunaan semula yang baik di mana secara purata, 99.4 ± 0.16 % HA pada UV_{254} dapat disingkirkan dengan

kadar 0.057 ± 0.004 min^{-1} sepanjang 10 kitaran ulang guna. Proses pemineralan MB and HA dibuktikan dengan analisis jumlah karbon organik (TOC) dan penurunan dalam nilai pH. Produk kimia yang terhasil daripada rawatan proses fotopemangkinan-penjerapan terhadap HA oleh P-25 TiO_2/2.0-O-MT-PVAB/GP dikenalpasti dengan analisis kromatografi cecair – spektrometri jisim (LC-MS). Kajian ini menunjukkan bahawa penggabungan fotomangkin dan bahan penjerap dalam bentuk dwilapisan adalah bermanfaat dan praktikal untuk penyingkiran sinergistik fotopemangkinan-penjerapan bahan pencemar organik daripada larutan akueus.

IMMOBILIZED P-25 TiO_2/MONTMORILLONITE AND P-25 TiO_2/ORGANO-MONTMORILLONITE BILAYER SYSTEMS FOR THE SYNERGISTIC PHOTOCATALYTIC-ADSORPTION REMOVAL OF METHYLENE BLUE AND HUMIC ACID FROM AQUEOUS SOLUTIONS

ABSTRACT

This research revolved around the development of immobilized P-25 TiO_2/montmorillonite and P-25 TiO_2/organo-montmorillonite bilayer systems for the synergistic photocatalytic-adsorption removal of methylene blue (MB) and humic acid (HA) from aqueous solutions. The initial stage of the development of the bilayer systems involved batch adsorption study of the sub-layer adsorbent. Immobilized montmorillonite (MT-PVAB/GP) was prepared for the adsorption of MB whereas immobilized organo-montmorillonite (2.0-O-MT-PVAB/GP) was fabricated for HA adsorption process. The MT-PVAB/GP and 2.0-O-MT-PVA were characterized by using field emission scanning electron microscopy (FE-SEM), energy dispersive x-ray (EDX), attenuated total reflectance-fourier transform infrared spectroscopy (FTIR-ATR), N_2 adsorption-desorption analysis and zeta potential measurements. The MB and HA adsorption processes were affected by adsorbent loading, solution pH, aeration rate, initial concentration and also, contact time. The kinetic data for adsorption of MB and HA were found to obey pseudo-second order kinetic model and intra-particle diffusion was the major rate limiting step for the adsorption processes. The adsorption isotherm study revealed that the MB and HA adsorption processes were best fitted with the Langmuir isotherm model. The maximum monolayer adsorption capacity, q_m of MT-PVAB/GP towards MB was 111 mg g^{-1}. Meanwhile, the q_m of HA adsorption at UV_{254} and $Colour_{436}$ was determined as

31.75 and 29.59 mg g^{-1}, respectively. The thermodynamic parameters values indicated that the MB and HA adsorption processes were favourable at higher temperature, endothermic and spontaneous. For the subsequent fabrication of the bilayer systems, the optimum composition of the sub-layer adsorbent of either MT-PVAB/GP or 2.0-O-MT-PVAB/GP and the upper layer P-25 TiO_2 was determined systematically by their synergistic photocatalytic-adsorption behaviour towards MB and HA, respectively. The optimized P-25 TiO_2/MT-PVAB/GP and P-25 TiO_2/2.0-O-MT-PVAB/GP bilayer systems were characterized by cross-sectional SEM, EDX, UV-vis diffused reflectance spectroscopy (UV-vis DRS) and photoluminescence spectroscopy (PLS). The synergistic photocatalytic-adsorption activity of the bilayer systems were primarily driven by their adsorption capacities which in turn were manipulated by solution pH, aeration rate, initial concentrations; higher separation rate of photo-generated electron-hole pairs and lower band gap energy as compared to the monolayer P-25 TiO_2/GP system. The UV irradiance intensity also affected the photocatalytic activity of the bilayer systems. The P-25 TiO_2/MT-PVAB/GP displayed enhancement in the synergistic photocatalytic-adsorption removal rate by 3.51 folds as compared with P-25 TiO_2/GP. Moreover, the P-25 TiO_2/MT-PVAB/GP bilayer system was highly reusable whereby on the average, the P-25 TiO_2/MT-PVAB/GP managed to remove 99.7 ± 0.14 % of MB at the average rate of 0.123 ± 0.006 min^{-1} throughout the 10 cycles of reuse. On the other hand, the P-25 TiO_2/2.0-O-MT-PVAB/GP demonstrated increase in the synergistic photocatalytic-adsorption removal rate of HA at UV_{254} by an average of 2.10 and 3.34 folds in comparison to P-25 TiO_2/MT-PVAB/GP and P-25 TiO_2/GP, respectively. The P-25 TiO_2/2.0-O-MT-PVAB/GP bilayer system also exhibited good reusability where on the average, 99.4 ± 0.16 % of HA at UV_{254} was eliminated with the average rate of 0.057 ± 0.004

min^{-1} during the 10 cycles of repeated applications. The photo-mineralization of MB and HA were reflected by total organic carbon (TOC) analysis and reduction in pH values. The HA intermediate products formed during the photocatalytic-adsorption process by P-25 TiO_2/2.0-O-MT-PVAB/GP were identified by liquid chromatography – mass spectrometry (LC-MS) analysis. This research demonstrated that the combination of photocatalyst and absorbent in an immobilized bilayer manner is advantageous and feasible for synergistic photocatalytic-adsorption removal of organic pollutants from aqueous solution.

CHAPTER ONE

INTRODUCTION AND LITERATURE REVIEWS

1.1 Background

In many countries, adverse climatic changes, rapid population growth compounded with industrialization and urbanization, limited water resources as well as a disproportion between socioeconomic development and water availability have resulted in a significant increase in the demand for water supply (Becerra-Castro *et al*., 2015, Vajnhandl and Valh, 2014). Dependence on natural water resources i.e. surface and ground water solely is insufficient to meet this rapidly growing demand, especially when an increasing number of water resources are experiencing over exploitation and anthropogenic pollution (Postigo and Barceló, 2015, Ribeiro *et al*., 2015). This critical situation has driven many authorities to seek for alternative or non-conventional water resources. In this context, treated wastewater has been identified as one of the most viable reclaimed water resource, particularly in countries situated in arid and semi-arid areas where water sources are short in supply (Pedrero *et al*., 2010). The introduction of treated wastewater as alternative source provides ecological goodness, diversifies water supplies and concurrently reduces contamination by minimizing wastewater in the environment (Mo and Zhang, 2013). So far, areas with water shortages have adopted treated wastewater mainly for irrigation purposes (Agrafioti and Diamadopoulos, 2012, Almuktar *et al*., 2015). The potential usages of treated wastewater for other means rely on the effectiveness of the treatment as the water quality of the reclaimed water are an important issue. The concern for health safety has called for stringent regulations upon the water quality of the treated wastewater, mainly for chemical compositions and microbial levels.

Hence, effective treatment methods are required to ensure compliance with the safety standards legislated for specific reuse purposes.

At present, most water and wastewater treatment plants employ traditional physicochemical and biological treatment methods such as coagulation-flocculation, sedimentation, ultra-filtration, disinfection and ozonation to purify and recover water. However, these conventional techniques have proved to be ineffective nowadays as the usages of numerous chemicals in the treatment systems may be hazardous and might result in the production of harmful by-products (Sarkar *et al*., 2007). Moreover, as a result of human activities, water resources are becoming polluted with trace and emerging organic contaminants such as pesticides, insecticides, pharmaceutical residues, industrial substances, personal care products and so on from industrial effluents or agricultural runoff which are difficult to be discarded by the conventional treatment methods (Fujioka *et al*., 2013, Sarkar *et al*., 2007). Other apparent weaknesses of conventional treatment methods include low removal of organic matter which induces the occurrence of algae and microorganisms in the distribution system (Escobar *et al*., 2000), ineffectiveness of combating outbreaks of recalcitrant bacteria (Khaldi *et al*., 2011), production of large amount of sludge during the water softening processes (Cheng *et al*., 2014) and the generation of potentially carcinogenic disinfection by-products (Doederer *et al*., 2014). Consequently, the applications of presently available water treatment technologies for recovery of wastewater effluent to produce high quality water are still bombarded with various ecological, technical and economical problems. Inevitably, this has urged extensive research in establishing judicious advanced treatment technologies in order to address such intrinsic shortcomings and subsequently meet the quality requirements for reusable as well as potable water.

1.2 Advanced Oxidation Processes (AOPs)

The water effluent generated by the multiple processes in conventional wastewater treatment methods may contain minimal levels of micro-pollutants and can even be potentially appropriate for reuse, especially for non-potable purposes (De Luca *et al*., 2013). However, in order to broaden the applicability of treated wastewater, the incorporation of more advanced treatment technologies as additional treatment is feasible for mineralization of the micro-pollutants or at least by converting them into less deleterious substances.

Advanced oxidation processes (AOPs) can be generally regarded as aqueous phase oxidation process based on production of highly reactive and transient species (normally hydroxyl radicals (•OH) with standard reduction potential, E° = 2.80 V vs. SHE) that can indiscriminately attack and destruct contaminants, yielding CO_2, H_2O or other innocuous by-products (Karci *et al*., 2013). In this chemical oxidation process, when the contaminants and their transitional products are totally destroyed, accretions of secondary wastes are prevented and hence, post-treatment is not required (Andreozzi *et al*., 1999). AOPs involve a series of superior and clean technologies for water treatment which mainly employ ultraviolet (UV) light, hydrogen peroxide (H_2O_2), ozone (O_3), oxygen (O_2) and vacuum (V), among others. Typical AOPs can be categorized as homogeneous and heterogeneous processes, depending on whether the processes involve a single phase or they utilize heterogeneous catalysts such as semiconductor in which its phase differs from that of the reactants. Major types of homogeneous AOPs are (a) photolysis which involves the direct use of UV light irradiance (Mihas *et al*., 2007); (b) O_3 based reactions which include O_3, O_3/UV (Latifoglu and Gurol, 2003), O_3/H_2O_2 and $O_3/UV/H_2O_2$; (c) wet peroxide oxidation which utilizes H_2O_2 as an oxidizing agent (Doskočil *et al*.,

2014); (d) the Fenton processes, namely the established Fenton H_2O_2/Fe^{2+} (Wu *et al*., 2010), H_2O_2/Fe^{3+}, $UV/H_2O_2/Fe^{2+}$ (Katsumata *et al*., 2008), sono-Fenton (ultrasound/H_2O_2/Fe^{2+}), electro-Fenton, photo-sono Fenton and photo-electro Fenton and (e) wet oxidation which occurs at high temperature (470-600K) and pressure (20-200 bar) and dissolved oxygen is applied as an oxidizing agent (Urrea *et al*., 2014). On the other hand, heterogeneous AOPs comprise of (a) heterogeneous photocatalysis where a semiconductor photocatalyst is activated in the presence of UV and/or visible light irradiance (Rajca and Bodzek, 2013, Valencia *et al*., 2013); (b) catalytic wet peroxide oxidation, which operates at temperatures between 323 to 353K (Gomes *et al*., 2010); (c) catalytic ozonation in which heterogeneous catalyst is employed to enhance the generation of highly reactive radicals, resulting in increased mineralization rates (Turkay *et al*., 2014); (d) heterogeneous Fenton-like processes such as H_2O_2/solid ($Fe^{2+}/Fe^{3+}/m^{n+}$) and H_2O_2/zero valent iron (Nie *et al*., 2010) and (e) catalytic wet oxidation in which as compared to the non-catalytic wet oxidation, the presence of catalyst permits the process to operate at milder temperatures (400-520 K) and pressures (5-50 bar) (Yadav and Garg, 2014).

Despite undergoing diverse pathways based on different fundamentals, the aforementioned AOPs are all characterized by the same chemical feature, which is the production of highly reactive and non-selective species such as •OH radicals in their overall mechanisms (Malato *et al*., 2009). These reactive species would lead to the oxidation destruction of persistent and non-biodegradable contaminants to harmless by-products or inert end products. Thus, the effectiveness of the varying AOPs allows one to select the appropriate AOP to specifically achieve the targeted water treatment requirements.

1.2.1 Applications of AOPs in water and wastewater treatment

The treatment limitations preceded by conventional and biological water treatment methods, especially for industrial wastewater treatment, have spurred extensive research on AOPs in search of more effective and sustainable water treatment technologies. Over the years, environmental applications of AOPs in water and wastewater treatment have been investigated on wastewater effluents produced from various industries such as textiles, pharmaceuticals, cosmetics, plastics, pesticides, herbicides, electronics and so on, which contain perilous and less biodegradable substances, namely antibiotics, cyanides, phenols, xenobiotics, ketones, alcohols, acetates, chlorinated and aromatic compounds (Badawy *et al*., 2006, De Luca *et al*., 2013, Elmolla and Chaudhuri, 2010, Kepa *et al*., 2008, Klavarioti *et al*., 2009). Other related environmental applications of AOPs include soil treatment, conditioning of solid sludge and removal of volatile or semi volatile organic pollutants.

By contemplating the magnitude of contamination and the targeted treatments, the implementation of AOPs for water treatment can be done solely or as practical support to complement the conventional physicochemical and biological treatment via combined processes. The integrated systems have been regarded as a feasible solution to overcoming the technical challenges of physical, chemical and biological processes by themselves as well as to minimize operation costs (Rodrigues *et al*., 2014). The AOPs have been engaged as pre-treatment to enhance the biodegradability of the initially persistent organic compounds, which would then follow by the biological oxidation process. During the pre-treatment by AOPs, the biologically persistent components of the compounds are partially oxidized to form biodegradable reaction intermediates. Meanwhile, the applications of AOPs as post-

treatment depict the removal of the biodegradable part of the wastewater as a preparatory step for subsequent treatment of the persistent or inhibitory pollutants by chemical oxidation processes. So far, studies on the combined systems of AOPs and biological process have been carried out for the elimination of phenol, formaldehyde, kraft pulp mill effluent, winery wastewater, pesticides, herbicides and synthetic textile dyeing wastewater (Lafi and Al-Qodah, 2006, Méndez *et al*., 2015, Merayo *et al*., 2013, Rodrigues *et al*., 2014, Sanchis *et al*., 2013, Souza *et al*., 2013).

Amongst the AOPs, heterogeneous photocatalysis has demonstrated to be very effective for pollutant abatement and water purification. The major advantages of heterogeneous photocatalysis are the semiconductor photocatalysts can be easily acquired, stable, reusable and there are continuous efforts to improve the reproducibility of the catalysts for long term application. In addition, heterogeneous photocatalysis process has the ability to remove a wide range of pollutants dissolved in aqueous medium and converts them into innocuous compounds. Furthermore, solar irradiation can be employed as a renewable energy source to initiate chemical reactions of heterogeneous photocatalysis.

1.3 Semiconductor induced heterogeneous photocatalysis

The process of heterogeneous photocatalysis basically refers to the chemical transformation reactions prompted by the occurrence of light energy and catalyst. In the case of semiconductor induced heterogeneous photocatalysis, the catalysts required in this process correspond to semiconductors which are responsive towards the irradiation of light. The reactions transpire due to the certain changes in the monomeric numbers N, the total energy levels, in the electronic structure of a semiconductor from atomic orbital to clusters. The band electronic structure of a

semiconductor is made up of the highest filled band (the valence band) and the lowest unfilled band (the conduction band) which are separated by a band gap, E_{bg}, a region representing an energy level in a crystallite state and is usually measured in unit of electron volt, eV. In order to initiate photocatalytic reactions, activation of a semiconductor photocatalyst is achieved by its interaction with light of sufficient energy, resulting in the promotion of electrons, e^- from the valence band to the conduction band with the simultaneous formation of holes, h^+ in the valence band. The photo-generated electron-hole pairs consequently either react with electron donors or acceptors through different interfacial processes or undergo recombination process. In order to allow successful production of reactive oxidizing species, these processes must compete with each other in an efficient manner (Mills and Hunte, 1997). The processes undertaken by the photo-generated electron-hole pairs can be depicted by the following equations (Robertson, 1996):

Absorption of light	Semiconductor $\xrightarrow{h\nu > E_{bg}}$	$e^-_{cb} + h^+_{vb}$	(1.1)
Recombination	$e^-_{cb} + h^+_{vb}$ $\longrightarrow$	heat	(1.2)
Oxidation	$D + h^+$ $\longrightarrow$	$D^{\bullet+}$	(1.3)
Reduction	$A + e^-$ $\longrightarrow$	$A^{\bullet-}$	(1.4)

The band positions of several semiconductors and their respective band gap energies are illustrated in Figure 1.1. The bottoms of the conduction band and the tops of the valence bands are shown along with their band gap in eV. The reactivity of the light mediated process depends greatly on the band positions. In order to attain redox reaction, the lower edge of the conduction bands has to be situated at a more negative potential than the reduction potential of the chemical substances that will be reduced while the upper edge of the valence bands must be placed more positively than the oxidation potential of the chemical substances that will be oxidized. Hence,

the minimum photon energy needed for activation of a semiconductor is the difference between the energies of the bottom of the conduction band and the top of the valence band (Melo and Silva, 2011). In semiconductor induced photocatalysis, the photo-chemical reactions mainly occur in two ways: (a) generation of highly reactive species resulted from the oxidation of hydroxide ions and reduction of oxygen, which would initiate reactions with the pre-adsorbed substrates at the solution interface and (b) direct oxidation or reduction of substances that migrate from the bulk solution to the surface of the semiconductor by the photo-generated electron-holes pierce (Taghizadeh *et al*., 2000). Similarly, in water remediation, the photo-generated holes and the formed hydroxyl radicals oxidize the nearby organic pollutants on the photocatalyst surface while the electrons in the conduction band are normally involved in reduction processes, which typically react with molecular oxygen to produce superoxide radical anions ($O_2^{\bullet-}$), another reactive oxidizing species.

The intense research and development of the applications of semiconductor mediated heterogeneous photocatalysis was triggered by the discovery of photo-induced water splitting on titanium dioxide (TiO_2) electrodes by Fujishima and Honda in 1972 (Fujishima *et al*., 1969, Fujishima and Honda, 1972). In the study, it was found decomposition of water into oxygen and hydrogen was possible upon the illumination of a n-type semiconductor TiO_2 under UV light ($\lambda < 415$ nm) without the use of external electrical supply. Since then, extensive studies have been conducted on the utilization of photocatalytic materials to transform solar energy into chemical energy for production of beneficial materials such as hydrogen (Fujishima and Honda, 1972, Kudo and Miseki, 2009, Maeda, 2011) and hydrocarbons (Inoue *et al*., 1979, Tahir and Amin, 2013b). The application of heterogeneous photocatalysis

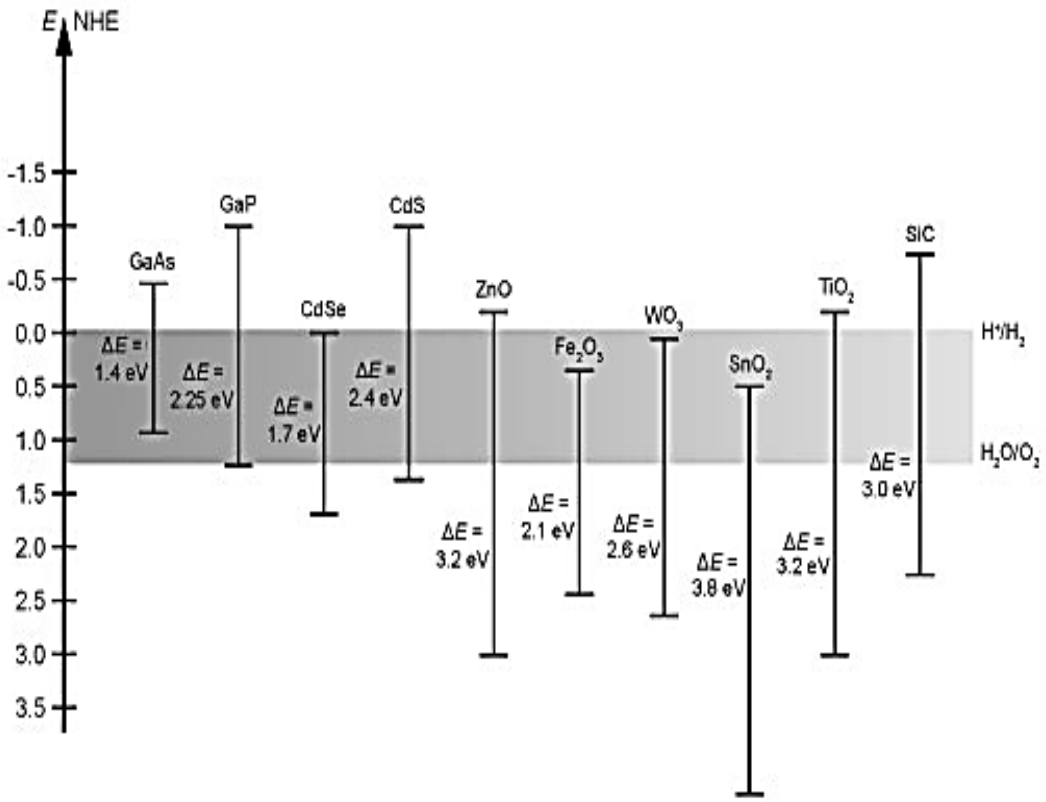

Figure 1.1: Valence and conduction band positions of some of the commonly studied semiconductor photocatalysts in contact with aqueous solution at pH 1 and their respective band gap energies (Melo and Silva, 2011).

for environmental cleanup was first initiated in 1977 by Frank and Bard who reported on the reduction of cyanide in water by illuminated TiO_2 powders (Frank and Bard, 1977a, Frank and Bard, 1977b). This marked the beginning of many intensive works in this area because of the prospective of utilizing the ‘’free’’ solar energy for water and air remediation.

Many semiconductors have been actively studied for photocatalytic environmental treatment, including TiO_2 (De la Cruz *et al*., 2013, García-Fernández *et al*., 2015, Nakata and Fujishima, 2012), ZnO (Xie *et al*., 2011, Song *et al*., 2014), Fe_2O_3 (Karunakaran and Senthilvelan, 2006), WO_3 (Szilágyi *et al*., 2012), CdS (Huang *et al*., 2011), CdSe (Meng *et al*., 2012), SnO_2 (Cheng *et al*., 2011), SiC (Zhang *et al*., 2014), ZnSe (Feng *et al*., 2014) and ZrO_2 (Jiang *et al*., 2014), among

others. With the aim of amplifying the reactivity of the photocatalytic reactions, two or more semiconductors are integrated and modified for enhanced removal of contaminants (Guo *et al*., 2014, Li and Haneda 2003, Liao *et al*., 2004). Despite the prolific availability of semiconductors, most of the photocatalytic studies are manipulated by the application of TiO_2 as the photocatalyst.

1.4 Structures and properties of TiO_2

The TiO_2 is basically of n-type semiconductor due to the presence of oxygen vacancies in its lattice (Wisitsoraat *et al*., 2009). The TiO_2 exists as three different polymorphs in nature; anatase (tetragonal), rutile (tetragonal) and brookite (orthorhombic) (Nolan *et al*., 2009). In all three forms, titanium (Ti^{4+}) atoms are co-ordinated differently to six oxygen (O^{2-}) atoms by vertices and edges, forming distorted TiO_6 octahedra (Paola *et al*., 2008). Anatase can be viewed as a tetragonal structure (space group $I4_1/amd$ with a = 3.782 Å and c = 9.502 Å) (Burdett *et al*., 1987) resulted from each octahedron sharing its four edges with the other four octahedrons (Figure 1.2(a)). In rutile, the tetragonal structure (space group $P4_2/mnm$ with a = 4.587 Å and c = 2.954 Å) (Burdett *et al*., 1987) is formed from the sharing octahedral edges along the direction of 001 plane (Figure 1.2(b)) while for brookite, both the vertices and edges are shared to provide an orthorhombic structure (space group P_{cab}, with a = 9.184 Å, b = 5.447 Å and c = 5.145 Å) (Figure 1.2(c)) (Wyckoff, 1963).

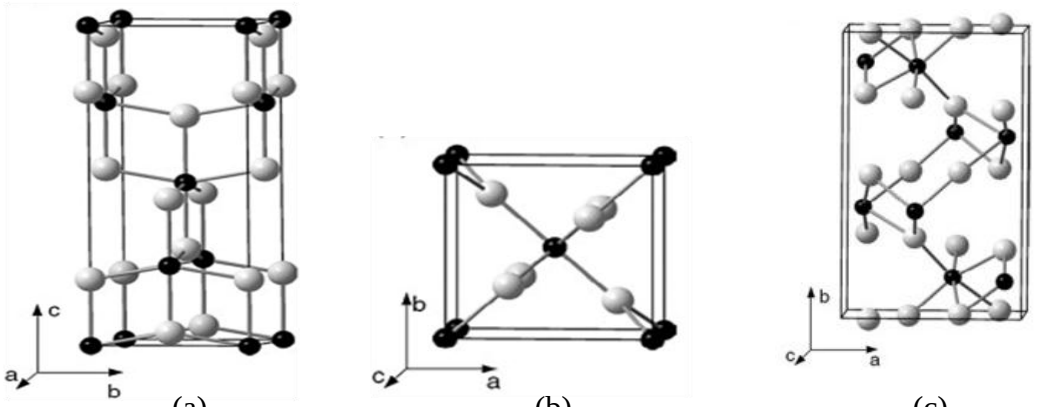

(a) (b) (c)

Figure 1.2: Bulk crystalline structures of (a) anatase, (b) rutile and (c) brookite form of TiO_2 (Janisch *et al*., 2005).

These three polymorphs of TiO_2 can be readily produced in laboratory by varying the preparation conditions and typically, the metastable anatase and brookite are susceptible to transform into the thermodynamically stable rutile when calcined at temperature above 600 °C (Hu *et al*., 2003). The conversion of anatase and brookite to rutile is reconstructive and ensues without the occurrence of other metastable phases (Huberty and Xu, 2008). Each phase demonstrates distinct structures, optical properties, band gap, surface states and so on which govern their applications. The estimated band gap energy is 3.21 eV for anatase, 3.00 eV for rutile and 3.13 eV for brookite (Reyes-Coronado *et al*., 2008). Anatase phase of TiO_2 has been found effective for uses in solar cells (Umar *et al*., 2014) and photocatalytic reactions (Herrmann *et al*., 2002). In this perspective, anatase phase TiO_2 is usually regarded more active than the rutile phase, mainly due to its smaller grain sizes with higher surface area and low surface energy, higher density of localised states, better production of surface adsorbed reactive radicals and slower recombination of electron-hole as compared to the rutile phase (Hanaor and Sorrell, 2011, Yuangpho *et al*., 2015). Moreover, the anatase phase TiO_2 also possesses good adsorptive and absorptive properties of ultraviolet (UV) irradiation and can be easily synthesized

(Reyes-Coronado *et al*., 2008). On the other hand, there are scarce studies on the photocatalytic behaviour of the brookite as its phase stability is still undefined (Huberty and Xu, 2008).

1.4.1 Primary mechanism of TiO_2 photocatalysis

During photocatalysis, light of energy greater than the band gap energy of the semiconductor is needed to initiate excitation of an electron from the valence band to the conduction band. For anatase phase TiO_2, the band gap is 3.21 eV (Reyes-Coronado *et al*., 2008), thus UV light of ≤ 386 nm is required. The in depth mechanism of TiO_2 photocatalysis has been discussed in literatures (Herrmann, 1999, Fujishima *et al*., 2000, Schneider *et al*., 2014) and summarized by Robert and Malato, (2002). The absorption of photon promotes an electron to the conduction band (e^-_{CB}) producing a positive hole in the valence band (h^+_{VB}) (Eq. 1.5).

$$TiO_2 + h\nu\ (> E_{bg}) \longrightarrow h^+_{VB} + e^-_{CB} \quad (1.5)$$

These photo-generated charge carriers are subsequently trapped for 100 ps (shallow trap) to 10 ns (deep trap) in the TiO_2 lattice or they can recombine with each another in the range of 10-100 ns, releasing energy (Eq. 1.6) (Tachikawa *et al*., 2007). Alternatively, these charge carriers migrate to the surface of TiO_2 and undergo interfacial charge transfers with the adsorbates such as oxygen, hydroxyl ions or even organic substrates in the time scale of 100 ns and ms (Hoffmann *et al*., 1995). The charge transfer process either directly decomposes the organic substrates (Eq. 1.7, 1.8) or generates reactive oxidizing radicals, namely hydroxyl radicals and superoxides. The positive holes oxidize the surrounding water molecules or hydroxyl ions, leading to the formation of the very powerful oxidants •OH radicals (Eq. 1.9,

1.10). The hydroxyl radicals consequently oxidize and mineralize the organic substrates, producing H_2O, CO_2 and mineral acids (Eq. 1.11).

$$e^-_{CB} + h^+_{vb} \longrightarrow \text{energy} \quad (1.6)$$

$$R + e^-_{CB} \longrightarrow R^{\bullet -} \quad (1.7)$$

$$R + h^+_{VB} \longrightarrow R^{\bullet +} \quad (1.8)$$

$$H_2O + h^+_{VB} \longrightarrow \bullet OH + H^+ \quad (1.9)$$

$$OH^- + h^+_{VB} \longrightarrow \bullet OH \quad (1.10)$$

$$R + \bullet OH \longrightarrow \cdots\cdots\blacktriangleright \cdots\cdots\blacktriangleright H_2O + CO_2 + \text{mineral acids} \quad (1.11)$$

Meanwhile, the electrons in the conduction band react with the adsorbed molecular oxygen on the TiO_2 to generate superoxide radical anion $O_2^{\bullet -}$ (Eq. 1.12) that can further react with H^+ to form hydroperoxyl radical •OOH (Eq. 1.13) and subsequent electrochemical reduction may yield H_2O_2 (Eq. 1.14). The H_2O_2 may generate •OH via its reaction with the photo-generated electron (Eq. 1.15). Similar to •OH, these reactive oxygen species, $O_2^{\bullet -}$ and •OOH, can also lead to oxidative elimination of organic substrates (Eq. 1.16 and 1.17) (Zhu *et al*., 2005b).

$$O_2 + e^-_{CB} \longrightarrow O_2^{\bullet -} \quad (1.12)$$

$$O_2^{\bullet -} + H^+ \longrightarrow \bullet OOH \quad (1.13)$$

$$\bullet OOH + \bullet OOH \longrightarrow H_2O_2 + O_2 \quad (1.14)$$

$$H_2O_2 + e^-_{CB} \longrightarrow OH^- + \bullet OH \quad (1.15)$$

$$R + O_2^{\bullet -} \longrightarrow \cdots\cdots\blacktriangleright \cdots\cdots\blacktriangleright H_2O + CO_2 + \text{mineral acids} \quad (1.16)$$

$$R + \bullet OOH \longrightarrow \cdots\cdots\blacktriangleright \cdots\cdots\blacktriangleright H_2O + CO_2 + \text{mineral acids} \quad (1.17)$$

Nonetheless, it is believed that •OH and $O_2^{\bullet -}$ are the main oxidizing agents in photocatalytic reactions (Robert and Malato, 2002). These processes are illustrated in Figure 1.3.

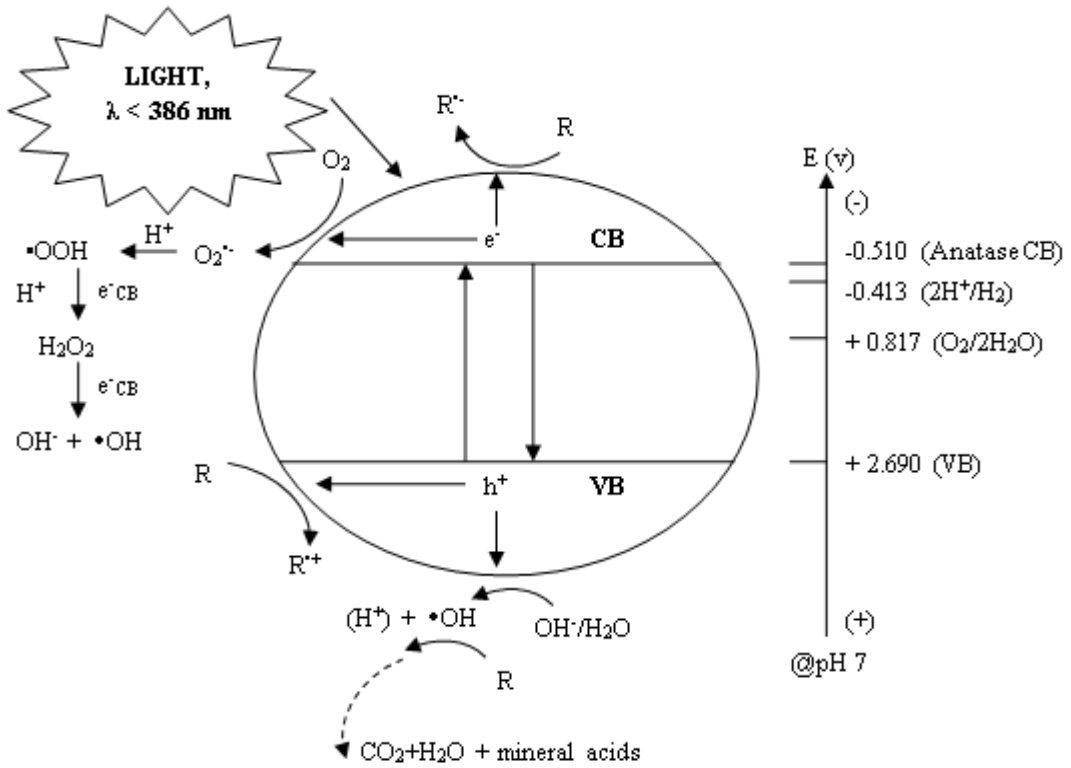

Figure 1.3: Schematic illustration for primary mechanism of TiO_2 photocatalysis (adapted from Park *et al.*, 2013).

1.4.2 Langmuir-Hinshelwood kinetics model

The kinetics for photocatalytic oxidation of many organic compounds is often explained by the Langmuir-Hinshelwood kinetics model. The derived kinetic model covers the adsorption properties of the substrate on the photocatalyst surface, the formation of charge carriers upon photo-excitation of a catalyst, recombination of the charge carriers, interfacial charge transfers that occur both on the surface and in the liquid which eventually lead to the elimination of the organic substrates (Turchi and Ollis, 1990). Based on this kinetic model, the rate of the reaction, *r*, is proportional to the portion of the surface covered by substrate, θ, as shown in the following Eq. 1.18 (Valente *et al.*, 2006):

$$r = -\frac{dC}{dt} = k_r\theta \tag{1.18}$$

where k_r is the limiting rate constant of reaction at maximum coverage under the given experimental conditions (mg L^{-1} min^{-1}). According to Langmuir's model, the adsorption on solid substrate can be described as in Eq.1.19.

$$\theta = \frac{KC}{1+KC} \tag{1.19}$$

Substituting Eq. 1.19, Eq. 1.18 becomes:

$$r = -\frac{dC}{dt} = k_r\theta = \frac{k_rKC}{1+KC} \tag{1.20}$$

In Eq. 1.20, K is the equilibrium constant for adsorption of the substrate onto the catalyst (mg^{-1} L) whereas C is the concentration at any time t during degradation (mg L^{-1}). After integration, Eq. 1.20 becomes:

$$\ln\left(\frac{C_o}{C}\right) + K\left(C_o - C\right) = k_rKt \tag{1.21}$$

where C_o is the initial concentration of the substrate and t is the reaction time. When the concentration of the substrates, C is reasonably high (C > 5 x 10^{-3} mol L^{-1}) and KC >> 1, Eq. 1.20 will be of zero order. On the other hand, when the concentration of the substrate is comparatively low at C < 10^{-3} mol L^{-1}, KC becomes << 1. Therefore, Eq. 1.20 describes an apparent first-order reaction as follows:

$$r = -\frac{dC}{dt} = k_rKC = k_{ap}C \tag{1.22}$$

where k_{ap} is the apparent rate constant of pseudo-first-order reaction. Eq. 1.22 can be integrated to give:

$$\ln\left(\frac{C_o}{C}\right) = k_{ap}t \tag{1.23}$$

By plotting $\ln\left(\frac{C_o}{C}\right)$ versus t, the apparent rate constant, k_{ap} can be determined from the slope of the plot (Behnajady *et al.*, 2006). The degree of agreement of the reactions with the Langmuir-Hinshelwood kinetic model is indicated by the coefficient of determination regression, R^2.

1.4.3 Applications of TiO_2 as photocatalyst

The great potential of TiO_2 mediated heterogeneous photocatalysis, as characterized by its ability to generate highly reactive radicals for total elimination of persistent pollutants, has gained significant attention. Among many semiconductors, TiO_2 is often considered as the most ideal photocatalyst mainly due to its non-toxicity, low cost, availability (Pekakis *et al*., 2006), applicability in UV and visible light region (Zhao *et al*., 2014), high oxidizing strength (Hoffmann *et al*., 1995), photo and chemical stability, super-hydrophilicity (Langlet *et al*., 2006), and ability to unselectively remove wide ranges of organic as well as inorganic contaminants in aqueous and gaseous media (Abbas *et al*., 2011, Satyro *et al*., 2014, Liao *et al*., 2014, Bianchi *et al*., 2015, Monteiro *et al*., 2015). Apart from water and air purification, TiO_2 photocatalysis has also been extensively researched for other environmental applications such as water splitting (Niu *et al*., 2013), dye-sensitized solar cells (Umar *et al*., 2014), self-cleaning (Castaño *et al*., 2014) and anti-fogging (Zeman and Takabayashi, 2002), predominantly due to its good photocatalytic properties. Despite the plentiful uses of TiO_2 photocatalysis, the development of system design and novel materials is strongly needed to produce amplified performance with respect to the photocatalytic properties as well as to unearth practical real scale applications for TiO_2 photocatalysis driven processes.

Due to its potential to mineralize broad range of persistent pollutants at ambient temperature and pressure into innocuous compounds, TiO_2 photocatalysis in slurry mode has emerged as the most advantaged and feasible approach in water and wastewater purification and detoxification processes (Rafqah *et al*., 2005, Affam and Chaudhuri, 2013). For the purpose of delivering high adsorption and photocatalytic efficiency, TiO_2 of small size particles is often employed due to its large specific

surface area (Jin and Dai, 2012). However, in practical applications, the operation system is inundated by critical technical limitations associated with agglomerations, suspensions or even floatation of fine powdered TiO_2, particularly at high concentrations, which causes adverse effect on their photocatalytic performances due to the reduction of their effective surface area (Wang *et al*., 2013a). In addition, the need for separation of fine TiO_2 catalysts from water at the completion of photocatalytic treatments can be energy intensive, time consuming, costly and can cause secondary pollution (Lei *et al*., 2012, Rottman *et al*., 2013). There have been suggestions that the release of TiO_2 nanoparticles to the environment may cause unwanted environmental and health hazard, due to their potential inflammatory and cytotoxic effects (Reijnders, 2008, Sun *et al*., 2012). Other technical problems that affect the viable application of suspended TiO_2 nanoparticles are the recovery, regeneration and reproducibility of the catalyst after the treatment. Realizing these constraints, many works have been devoted to the development of immobilized, anchored, embedded or dispersed TiO_2 nanoparticles onto inert or functional supports with large surface area, good porosity, high photo and chemical stability which not only overcome the call for complex separation processes as post treatment but also promote enhanced photocatalytic activities. Numerous TiO_2 immobilization techniques by means of sol-gel method (Guillard *et al*., 2002, Pagáčová *et al*., 2014), microwave hydrothermal treatment (Zhang *et al*., 2006), hydrothermal synthesis (Wang *et al*., 2013b), chemical vapour deposition (Sun *et al*., 2008), electrophoretic deposition (Nawi *et al*., 2003), thermal treatment (Radeka *et al*., 2014) and dip-coating (Nawi and Zain, 2012), among others have been reported. As most of the TiO_2 immobilization processes usually engage severe chemical and thermal

conditions, porous clay materials of highly stable structure coupled with superior adsorption properties are often in great demand as photocatalyst support.

1.5 Overview of clay minerals

In general, clay minerals can be referred as hydrated phyllosilicate minerals and minerals, which impart plasticity to clay and which harden upon drying or frying (Guggenheim and Martin, 1995). They appear as aggregates of particles, in which a particle consists of a group of ordering layers (Bergaya and Lagaly, 2006). Due to their abundance in nature and versatility, clay minerals have been extensively applied in agriculture, construction, industrial engineering, biological and environmental applications (Choy *et al*., 2007, Iglesias *et al*., 2014, Abidi *et al*., 2015). Among the many sorbents, clay minerals are frequently chosen as alternative adsorbents that offer many advantages in numerous applications. Firstly, clay minerals display very high surface area of about 800 mg^2 g^{-1} (Geyer *et al*., 2014) due to their lamellar structures, which permits the adsorption of compounds on the particle external sites and also within the interlayer regions (Errais *et al*., 2011). Other benefits of clay minerals as adsorbents include its low-cost, environmental friendliness, widespread availability, the presence of surface charges that allows the accumulation of cationic organic and inorganic contaminants as well as high ion exchange potential for charged pollutants (Gil *et al*., 2011). Clay minerals are also highly porous as micro-pores are formed between the interlayer spaces and macro-pores are resulted from the voids that are generated between the particles and between the aggregates of particles (Sedighi and Thomas, 2014). By incorporating various species into the interlayer spaces, their structural properties can be altered and this allows them to be applied as new functional materials. These modified clay minerals have shown wide

applications for adsorption and catalytic processes in environmental decontamination of many types of pollutants (Mirmohamadsadeghi *et al*., 2012, Djomgoue *et al*., 2012, Zhou *et al*., 2014, Sanabria *et al*., 2009, Vaccari, 1999). Due to their variety of surface and structural characteristics, an in-depth understanding of the physicochemical properties of clay minerals is essential to allow them to be directly applied or modified to accommodate specific remediation purposes.

1.5.1 Structure and properties of clay minerals

The diverse chemical and behavioural properties of clay minerals arise from their different charges, degree of net layer charge, layer structure arrangement and interlayer species (Martin *et al*., 1991). Based on their different charges, there are two main groups of clay minerals, namely cationic and anionic clays. The cationic clays have negatively charge alumina-silicate layers with small cations within the interlayer region to counterbalance the charge whereas the anionic clays possess positively charged metal hydroxide with anions and water molecules located interstitially for charge balancing. The cationic clays are mainly acquired from the natural minerals while the anionic clays are usually synthesized (Vaccari, 1998, 1999). As the cationic clays are ubiquitous in nature, they are widely applied as catalysts and sorbents for environmental remediation.

All cationic clay minerals are generally made up of two basic components arranged alternately to provide structures of different layer types. These two elementary building blocks of clay minerals consist of a tetrahedral sheet of silicate and an octahedral sheet of alumina, in which the tetrahedrally coordinated silica sheets are linked through shared oxygen to sheets of alumina octahedrally coordinated to oxygen and hydroxyls (Vaccari, 1998). The structures are

differentiated by the number of tetrahedral and octahedral sheets. When one tetrahedral sheet is attached to one octahedral sheet, it is classified as 1:1 phyllosilicates (Figure 1.4(a)), such as kaolinite and serpertine group. The structure made up of two tetrahedral sheets sandwiching one octahedral sheet is known as 2:1 phyllosilicates (Figure 1.4(b)), which include smectite, vermiculite, illite, chlorite, mica, palygorskite and sepiolite group (Carrado, 2004). Additionally, there are two types of octahedral sheets that exist in clay minerals depending on the number of cation sites in the octahedral sheet that are filled. If the octahedral sheet is mainly occupied by divalent cations (Mg^{2+}, Fe^{2+}), it demonstrates the trioctahedral character. Meanwhile, when about majority of the valid cation positions are taken up by trivalent cations (Al^{3+}, Fe^{3+}), it is of the dioctahedral series (Sparks, 1995, Jaber and Miehé-Brendlé, 2008).

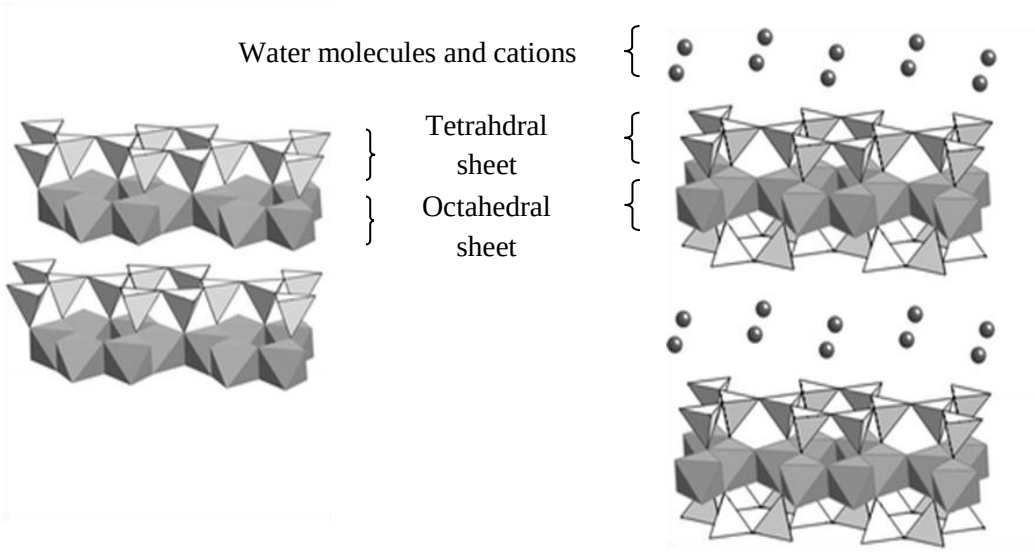

Figure 1.4: A structural diagram of (a) 1:1 and (b) 2:1 clay minerals (Hick *et al*., 2010).

The active sites of clay are affected by factors related to isomorphous substitutions, broken edges, lattice defects, cation exchange sites and layer net charge

(Moronta, 2004). The isomorphic substitution of Si^{4+} in the tetrahedral sheet or Al^{3+} or Mg^{2+} in the octahedral sheet generate negative charge on the clay surface. In tetrahedral sheet, Al^{3+} or occasionally Fe^{3+} can replace Si^{4+}. For dioctahedral minerals, the most usual substitution is Mg^{2+} for Al^{3+} and Li^{+} often replaces Mg^{2+} in trioctahedral minerals (Carrado, 2004). Isomorphic substitutions occur more often in the octahedral sheets. When the incoming cation has lower valence than that of the substituted cation, the lattice becomes negatively charged and this charge imbalance is compensated by the hydrated exchangeable cations (Na^{+}, K^{+}, Mg^{2+}, Ca^{2+}) in the interlayer (Vaccari, 1998). The interlayer cations are placed in the hexagonal openings guarded by two opposite tetrahedral sheets (refer to Figure 1.4 (b)). The magnitude of hydration differs depending on factors associated to the nature of cations and the composition of the layers (Meunier, 2005, Zheng *et al*., 2011, Salles *et al*., 2013). Such cations are typically exchangeable and their amount accounts for about 80 % of the total cation exchange capacity (CEC) of the clay minerals. The uncoordinated metal ions at the broken edges may react with the surrounding water molecules to form hydroxyls group such Si-OH and Al-OH which render the active sites of the clay to be protonated or deprotonated depending on the pH value of the media. The contribution of these edge sites to CEC is about 20 % and relies on the shape and size of the clay particles, whereby the contribution to the reactivity increases inversely with the particle size. The different magnitude of net layer charge resulted from isomorphous substitutions determines the exchangeability of the interlayer ions for various types of molecules, which can even change the clay nature from hydrophilic to organophillic. Low layer charges indicate that the interlayer ions are not firmly held and can be easily exchangeable (Moronta, 2004).

Currently, the most studied clay minerals for development of water and wastewater treatment technology are of the smectite group, primarily due to their high cation exchange capacity, propensity to macroscopic swelling and large specific surface area (Salles *et al*., 2013). These criteria are very important for developing functional adsorbents and supports for catalysts (Carriazo *et al*., 2010, Guerra *et al*., 2010, Liao and Kuo, 2007). The most common representative of smectite group is montmorillonite which is named after its location Montmorillon, France (Carrado, 2004).

1.5.2 Montmorillonite

Montmorillonite (MT) is a dioctahedral 2:1 phyllosilicates with particle size ranging from 0.1 - 2 μm in diameter and they are of irregular shape (Lagaly and Ziesmer, 2003). The octahedral sheets of MT are mainly resided by Al^{3+} but can be partially substituted by Fe^{2+} and Mg^{2+}. Isomorphous substitutions at the tetrahedral sheets of MT also occur, with some Si^{4+} replaced by Al^{3+}. The ideal formula per half unit cell of MT is $M_{0.33}$, $H_2OAl_{1.67}(Fe^{2+},Mg^{2+})_{0.33}Si_4O_{10}(OH)_2$, where M refers to a metal cation in the interlayer space between the sheets. The isomorphous substitutions of higher valence cations with lower valence cations cause MT to possess net negative charge. These negative charges can be balanced by hydrated exchangeable cations represented by $M_{0.33}$ (Sparks, 1995). The hydrated interlayer cations that a typical MT has are Na^+, Ca^{2+} or Mg^{2+} which are loosely held and easily exchanged with cations, giving rise to cation exchange capacity and simple sorption of cations from aqueous solutions via ion exchange. MT also has the capability to accommodate large amounts of water and polar organic molecules between the layers, thus resulting in significant expansion of the interlayer spacing and causes

swelling (Moronta, 2004). The presence of multiple layers of water molecules can typically increase the basal spacing of the clay, varying from 10 - 20 Å (Corrado, 2004, Bongiovanni *et al*., 2006). The swelling components of MT provide high surface area for adsorption and concentration of organic substrates (Feuillie *et al*., 2013). Hence, the typical features acquired by MT such as large active surface area, high CEC, good internal swelling ability when in contact with water and good binding ability have witnessed wide utilization of MT based materials in water and wastewater treatment, namely for removal of metal ions (Abollino *et al*., 2008, Wu *et al*., 2011, dos Anjos *et al*., 2014), dyes (Elsherbiny, 2013, Bhattacharyya *et al*., 2014), flocculation (Rulyov *et al*., 2000), coagulation (Assaad *et al*., 2007, Lagaly and Ziesmer, 2003), etc. These attributes of MT also allow them to undergo various modifications by different surface treatments such organo-montmorillonite (O-MT) (Zhou *et al*., 2008), acid-alkali treatments (Bhattacharyya and Gupta, 2008), polymer grafting (Liu, 2007) and thermal treatment (Fernández *et al*., 2013), among others in order to expand the applicability of MT as environmental remediation material.

1.5.3 Organo-montmorillonite

As discussed earlier, the isomorphic substitution of Al^{3+} for Mg^{2+} or Fe^{2+} at the octahedral sheet of MT and similar replacement of Si^{4+} by Al^{3+} at its tetrahedral sheet render a deficit of positive charge and thus, MT is negatively charged. The negative structural charge of MT is counterbalanced by exchangeable cations such as Na^{+}, Ca^{2+} and so on. Consequently, MT adsorbs ions and polar molecules efficiently but the utilization of MT for removal of non-polar organic molecules, on the contrary, is less effective (Liu *et al*., 2008a).

Surface modification by replacing the interlayer exchangeable cations with cationic surfactants is one of the most viable ways to alter the surface characteristics of MT (Bergaya and Lagaly, 2001). O-MT is typically synthesized by intercalating cationic surfactants such as quarternary ammonium compounds ($[(CH_3)_3NR]^+$ where R is alkyl hydrocarbon) onto the interlayer regions of the MT via cation exchange mechanism. The cation exchange reaction rate can be influenced by temperature, density of interlayer charges, size and valence of exchangeable cations and mutual interaction between alkyl chains (Slade and Gates, 2004, Lee *et al*., 2005, Gammoudi *et al*., 2012). When the interlayer regions of MT are saturated with larger monovalent cations such as K^+, Rb^+, NH_4^+, Cs^+ which possesses low hydration energies, the strength of the electrostatic attraction between the layers is very strong and thus, mobility of the exchangeable cations is limited. On the other hand, when the interlayers are saturated with smaller cations such as Na^+, Li^+ Ca^{2+}, Mg^{2+} which are highly hydrated, the attraction between the interlayers can be overcome and the basal spacing of the clay will be enhanced (Laird, 2006). This allows the exchangeable cations to be more mobile and easier to be substituted by the organic cations. Due to the presence of hydrated exchangeable cations and adsorption of water molecules within the interlayer, the montmorillonite is predominantly hydrophilic prior to the intercalation of organic cations. This explains the ineffectiveness of unmodified montmorillonite as adsorbents for hydrophobic organic compounds (Shah *et al*., 2013).

The most apparent outcome of replacing the inorganic cations with organic cations is that the montmorillonite surface will become hydrophobic (Hongping *et al*., 2004). The interactions between the organic cations are often linked to the active sites of montmorillonite surfaces such as isomorphic substitutions positions, broken